Impact of Gate Oxide Thickness Variations on Hot-Carrier Degradation

S.E. Tyaginov[1,2], I.A. Starkov[3], O. Triebl[1,4], M. Karner[4], Ch. Kernstock[4], C. Jungemann[5], H. Enichlmair[6], J.M. Park[6], and T. Grasser[1]
[1]Institute for Microelectronics, TU Wien, Gußhausstraße 27-29, A-1040 Vienna, Austria.
[2]A.F.Ioffe Physical-Technical Institute, 26 Polytechnicheskaya Str., 194021 St.-Petersburg, Russia.
[3]Christian Doppler Laboratory for Reliability Issues in Microelectronics at the Institute for Microelectronics, TU Wien, Gußhausstraße 25-29, A-1040 Vienna, Austria.
[4]GlobalTCADSolutions GMBH, Graumanngasse 7, Stiege B/5 Stock, 1150 Wien.
[5]Institute für Theoretische Elektrotechnik, RWTH Aachen, 52056 Aachen, Germany.
[6]Process Development and Implementation Department, Austriamicrosystems AG, Unterpremstaetten, Austria.
Phone: +43-1-58801-36025. Fax: +43-1-58801-36099. Email: tyaginov@iue.tuwien.ac.at

***Abstract*-We analyze the impact of oxide thickness variations on hot-carrier degradation. For this purpose, we develop an analytical approximation of our hot-carrier degradation (HCD) model. As this approximation is derived from a physics-based model of HCD, it considers all the essential features of this detrimental phenomenon. Among them are the interplay between single- and multiple-carrier mechanisms of interface state creation as well as the strong localization of the damage near the drain end of the gate. Both single- and multiple-carrier processes are controlled by the carrier acceleration integral which is calculated using information on the carrier energy distribution function. In the TCAD version of the model these functions are obtained from a solution of the Boltzmann transport equation by means of the Monte-Carlo method, which is computationally very expensive. To avoid that, an analytical expression which represents the carrier acceleration integral has been proposed. This expression provides an analytical dependences of the interface state density and the linear drain current change vs. time. Moreover, it allows us to incorporate the impact of variations in device architectural parameters on the acceleration integral and, hence, on HCD. As an example, we apply this strategy to describe the effect of variations in the oxide thickness on the linear drain current degradation (ΔI_{dlin}) during a hot-carrier stress. We demonstrate that the oxide thickness change substantially impacts ΔI_{dlin} in a wide range of stress times.**

I. Introduction

It is commonly accepted that hot-carrier degradation (HCD) is a strongly localized phenomenon [1-3] as the density of interface states (N_{it}) produced by channel carriers peaks near the drain edge of the gate. This is because carriers need to pass some distance in the electric field before they are accelerated up to energies high enough to efficiently trigger Si-H bond-breakage. Additionally, the electric field itself is non-uniformly distributed and demonstrates the maximum near the pinch-off region.

In order to capture this non-locality, different quantities have been considered as the driving force of this detrimental phenomenon. Among them are the electric field, carrier average energy, carrier dynamic temperature, etc [4,5]. The peak position of the interface state density profile $N_{it}(x)$ (where x is the coordinate along the Si/SiO_2 interface) is thereby related to the maximum of this particular quantity indicating the degradation severity. Since in all cases the driving force of HCD is a distributed quantity, the shape of the interface state density lateral profile $N_{it}(x)$ is defined by the device architecture.

In our previous works [6,7] we demonstrated that the $N_{it}(x)$ peak is best defined by the carrier acceleration integral (AI) and is shifted with respect to the maxima of other quantities used as HCD driving force. The acceleration integral is a macroscopic quantity which characterizes the cumulative ability of the carrier ensemble to rupture a Si-H bond. The AI is obtained by multiplication of the carrier energy distribution function weighted with the density-of-states and the carrier velocity by the Si-H dissociation reaction cross section followed by integration over the energy. Therefore, each carrier observed in and characterized by certain energy makes a contribution to the bond dissociation process. The key ingredient in this modeling strategy is the carrier distribution function which is evaluated in each point at the Si/SiO_2 interface for particular device architectures.

As such, the topological features of a concrete device such as the doping profiles, oxide thickness, gate extension, etc. can strongly affect the device life-time under hot-carrier stress. At the same time, these architectural peculiarities vary from device to device even in the case when these devices are fabricated within the same technological cycle [8]. As a result, it is expected that such fluctuations can impact the device characteristics degradation. In this work, we employ our analytical approach to hot-carrier degradation modeling [9] to analyze the impact of the oxide thickness (d_{ox}) variations on hot-carrier degradation.

II. Model and Parameterization

Our analytical approach to HCD simulation is directly obtained from our physics-based TCAD model [6,7]. The model relies on a thorough solution of the Boltzmann transport equation by means of the Monte-Carlo approach. For this purpose we use a full-band Monte-Carlo device simulator MONJU [10] which calculates the carrier distribution function at the transistor interface for a given device architecture. Such an approach allows to naturally capture the main peculiarities of

hot-carrier degradation. First, since the model relies on the distribution function we can incorporate both "colder" and "hotter" carrier into the Si-H bond dissociation kinetics. Second, "hotter" carriers trigger the single-carrier process of HCD while colder counterparts contribute to the multiple-carrier process of interface states creation. As a consequence, the model considers the interplay between these two modes of Si-H bond-breakage. Finally, in our modeling framework the driving force of the damage is the carrier acceleration integral. And the maximum of the AI is pronounced near the position where the carrier distribution function demonstrates most extended high-energy tails. Thus, the important feature of HCD, i.e. its strong localization, is also described by the model.

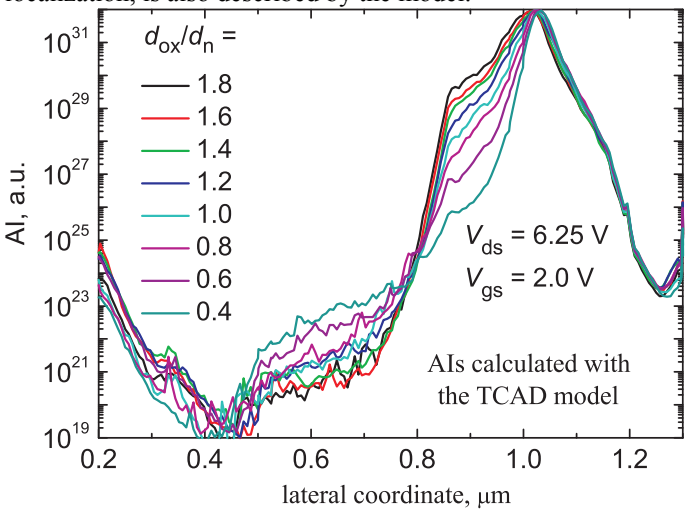

Fig. 1. The AI profiles calculated with the calibrated TCAD model for different oxide thicknesses (except d_{ox}, the device topology is same).

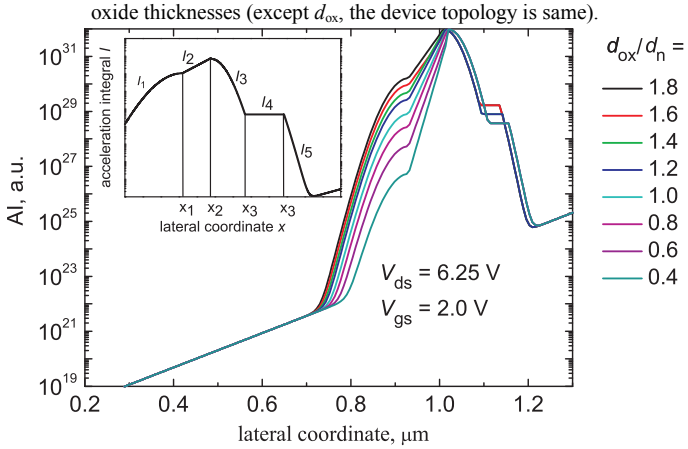

Fig. 2. The AI profiles calculated with the calibrated TCAD model for different oxide thickness (except d_{ox}, the device topology is same).

While deriving an analytical approach to HCD modeling we strove to keep all these features captured by the TCAD model. Since in our physics-based version of the model the quantity controlling the matter is the carrier acceleration integral, in the analytical approach we also deal with this value. The AI profile is represented by a fitting formulae, which gives an analytical expression for the linear drain current change with time $\Delta I_{dlin}(t)$, too. We recall that the acceleration integral profile $I(x)$ is expressed as a combination of the linear (in semi-log scale) dependence

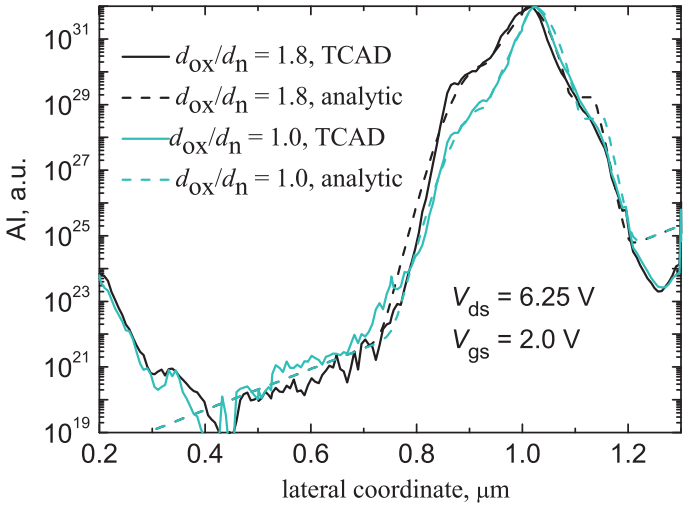

Fig. 3. Comparison between AIs calculated with the TCAD model and the analytical expression for two particular thicknesses.

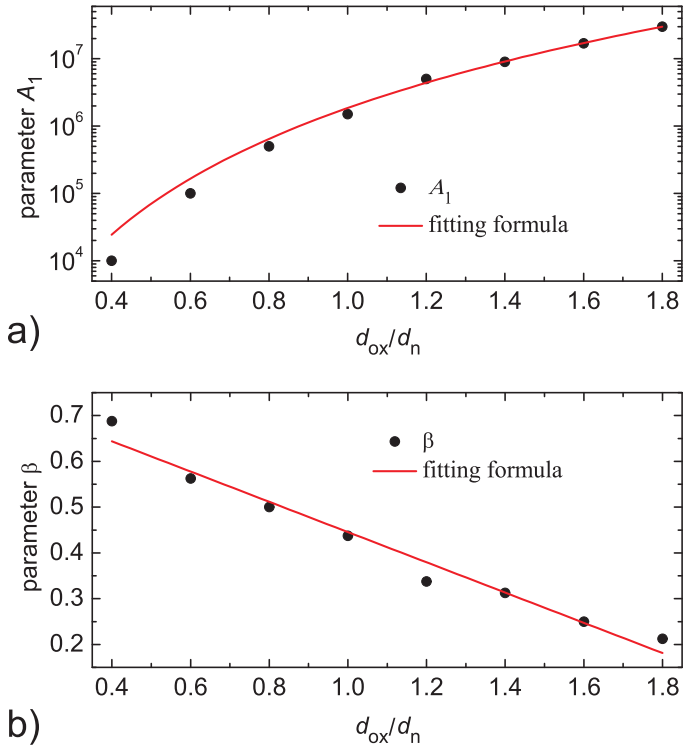

Fig. 4. Dependences of parameters A_1 (a) and β (b) on the relative oxide thickness d_{ox}/d_n.

$I_{linear}(x)$ and the peak term $I_{peak}(x)$, see Figs. 1-4 (more details are given in [9]):

$$I(x) = I_{linear}(x) + I_{peak}(x)$$
$$I_{linear} = A_1 \exp[\alpha(x - x_{min})] \quad (1)$$

The peak term is expressed as a combination of piecewise functions, i.e. $I_{peak}(x) = \Sigma I_i(x)$, see Fig. 2, inset:

$$F(x,<x>,A,\sigma)=A\exp\left(a\frac{\exp\left[\frac{x-\langle x\rangle}{\sigma}\right]}{\left(1+\exp\left[\frac{x-\langle x\rangle}{\sigma}\right]\right)^2}\right)$$

$$\begin{aligned}
&I_1=F(x,x_1,A_2,\sigma_1),x\le x_1\\
&I_2=A_2\exp\left[a\left(\frac{1}{4}+\beta(x-x_1)\right)\right],x\in(x_1;x_2]\\
&I_3=F(x,x_2,A_3,\sigma_2),x\in(x_2;x_3]\\
&I_4=I_3(x_3),x\in(x_3;x_4]\\
&I_5=F(x,x_5,A_4,\sigma_2),x\ge x_4,x_5=x_2+x_4-x_3
\end{aligned}\qquad(2)$$

With such a parameterization of the acceleration integral we calculate from the coordinate-dependent value of the interface state density $N_{it}(x)$ to an average value characterizing the degraded device in general. For the interface states created by the single-carrier process we assume first-order kinetics

$$\langle N_{it,SE}\rangle=N_0\left(1-\frac{1}{L_{int}}\int_{L_{int}}e^{-t\nu I(x)}dx\right),\qquad(3)$$

where N_0 is the concentration of Si-H bonds, L_{int} the length of the interface, and ν is a prefactor (attempt frequency). As for the multiple-carrier mechanism, in our high-voltage devices this process is already saturated, i.e. leads to coordinate independent N_{it} [7]. It is important to emphasize that with the fitting expression for the AI given in the form (2) integration in (3) leads to an analytical expression also for ‹$N_{it,SE}$› and, as a result, to an analytical formulae for ΔI_{dlin} vs. t (for more details see [6]).

In the TCAD version of our HCD model we used a combination of different device simulators in order to achieve a reasonable trade-off between the accuracy and computational burden [6-8]. First, the full-band Monte-Carlo device simulator MONJU is used to calculate the set of carrier distribution functions along the interface. Then, these distribution functions are used to calculate the carrier AI vs. x and eventually to produce the trap density as a function of the position at the interface, i.e. $N_{it}(x)$. Finally, the interface state concentration calculated in this manner is used as input for our device simulator MINIMOS-NT [12,13] to calculate the characteristics of the degraded device [6,7,11]. The whole computational procedure was performed for each time step in order to evaluate the degradation of device characteristics against the stress time.

A “brute-force” approach to analyze the impact of device architecture variations on the behavior of the transistor degraded during hot-carrier stress may be performed in the following manner: At the initial step a set of topologically identical devices differing only in the value of the fluctuating parameter is generated. Then, for each particular device (with the unique value of the varying parameters) the whole described procedure is to be applied. The results are then binned into histograms and statistically processed by weighting with the statistical distribution of the fluctuating quantity.

Due to stochastic nature of the Monte-Carlo approach, such a computational procedure, however, would lead to an enormous computational burden. And even more dramatic, if we vary this geometrical parameter with a reasonably small step, we should pay especial attention to the calculation accuracy. Otherwise, no prominent difference between results calculated for pretty similar (but still not identical) devices will be obtained. To summarize, all these circumstance make this “brute-force” strategy practically unrealistic.

Therefore, we use an analytical approach which is calibrated using the results obtained with the TCAD version of the HCD model. We vary an architectural parameter (in this paper the oxide thickness) and for some reference??? values we apply the full TCAD model to obtained exact dependences $\Delta I_{dlin}(t)$. Then we interpolate parameters in the analytical formula for the acceleration integral in order to cover the whole range of the fluctuating parameter.

We use a 5V n-MOSFET fabricated on a standard 0.35μm process with the nominal oxide thickness d_n = 148.26Å. The analytical model was calibrated to describe the linear drain current change under hot-carrier stress for the device with the oxide thickness fixed to d_n [7, 11]. The stress source-drain and source-gate voltages were V_{ds} = 6.25V and V_{gs} = 2.0, respectively. The stress was performed for 10^4s at room temperature.

To study the impact of oxide thickness variations on the linear drain current change due to hot-carrier ageing, we varied d_{ox} in a wide range from $0.4d_n$ to $1.8d_n$. Then for the reference values of d_{ox} (d_{ox}/d_n was 0.4, 0.6, 0.8, 1.0, 1.2, 1.4, 1.6, and 1.8) we performed the complete simulation scheme (including the time-consuming Monte-Carlo module) and calculated the AI profiles, see Fig. 1 (stress voltages were V_{ds} = 6.25V and V_{gs} = 2.0V).

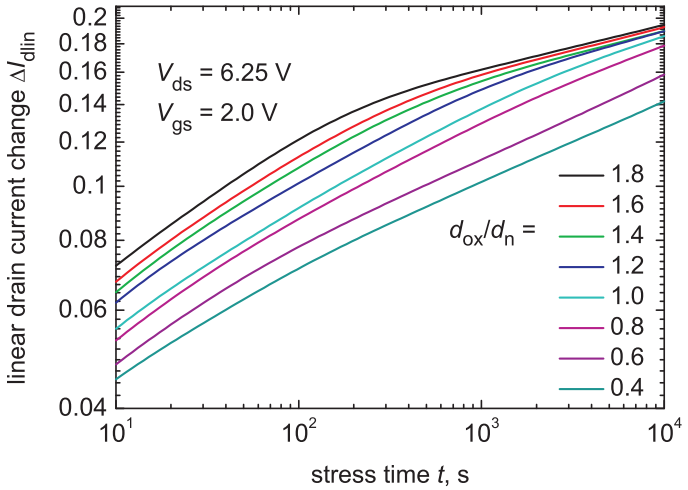

Fig. 5. Dependences $\Delta I_{dlin}(t)$ calculated for different values of d_{ox}.

Fig. 2 demonstrates the series of acceleration integrals calculated for varying d_{ox} using the analytical formula. The direct comparison between acceleration integrals for the thicknesses of $1.8d_n$ and $1.0d_n$ is shown in Fig. 3. From Figs. 1,2 one concludes that the slope of the right front of the AI (represented by fragments I_3, I_5, see Fig. 2, inset) remains the same (slight deviations in the shape of I_3, I_5 and the ledge I_4 boundaries are related to the statistical noise within the

Monte-Carlo approach). Therefore, the only varying parameters are the height of I_1 (parameter A_1) and the slope of I_2 (parameter β). We plotted these parameters as functions of the normalized oxide thickness, i.e. of d_{ox}/d_n, see Fig 4. In order to obtain the values of A_1 and β for the whole range of varying d_{ox}/d_n we represented their dependences $A_1(d_{ox}/d_n)$ and $\beta(d_{ox}/d_n)$ by fitting formulas (see Fig. 4 a,b):

$$A_1 = A_{1,0}\left(\frac{d_{ox}}{d_n}\right)^b; A_{1,0} = 1.85\cdot 10^6; b = 4.73$$
$$\beta = \beta_0 \frac{d_{ox}}{d_n} + \beta_1; \beta_0 = -0.33; \beta_1 = 0.78. \quad (4)$$

These expressions are further used for statistical analysis of ΔI_{dlin} in the case of a fluctuating d_{ox}.

III. Model and Parameterization

Using acceleration integrals from Fig. 2, a series of reference curves $\Delta I_{dlin}(t)$ was calculated for different values of d_{ox}, Fig. 5. One can see that $\Delta I_{dlin}(t)$ substantially changes as the oxide thickness varies. This change is especially pronounced for moderate stress times, i.e. less than 10^3s. For stress time larger than 10^3s the difference between ΔI_{dlin} obtained for various d_{ox} tends to saturate. For all gate oxide thicknesses the peak of the acceleration integral is pronounced at the same position and the fragment varying with d_{ox} is the left front of the AI. This varying front defines the difference between $\Delta I_{dlin}(t)$ at short stress times calculated for the devices with different d_{ox}.

Indeed, for these long-channel devices the mechanism dominating the Si-H bond dissociation is the single-carrier process. This process is triggered be really hot carriers (in contrast to the multiple-carrier process where several "colder" particles can provoke bond-breakage) [14.15]. Since for the single-carrier process first-order kinetics are assumed, the interface state density evolution vs. time is described by the activation exponent, i.e. $N_{it}(x,t) = N_0(1 - e^{-I(x)\nu t})$. Therefore, a trap is assumed to be activated when the condition $I(x)\nu t \sim 1$ is satisfied. With $\nu = 1.2\cdot 10^{-32}$ this conditions means that interface states that are created within 10^3s correspond to $I(x)$ of $\sim 10^{29}$ and higher. For longer stress times dissociation of bonds located at coordinates with $I(x) < 10^{29}$come into play. At the same time, as we already mentioned, variations in d_{ox} affect only the left front of the AI with the values just less than 10^{29}.

For the same reason, the distance between curves $\Delta I_{dlin}(t)$ obtained for various d_{ox} after some time starts to disappear). This trend is more pronounced (or occurs earlier) for thinner oxide films. Lower d_{ox} corresponds to higher peak values of the acceleration integral. And such high values mean that all available Si-H bonds are predominately broken independently of the particular value of the AI and, hence, on the particular oxide thickness. As a result, the difference between $\Delta I_{dlin}(t)$ curves tends to vanish at $t \sim 10^4$s.

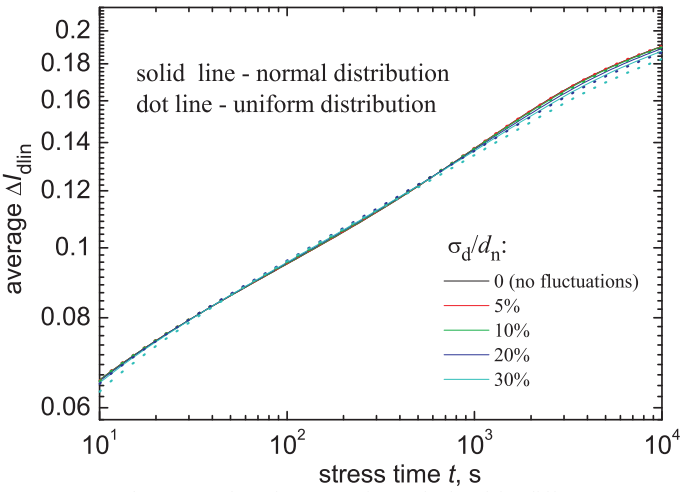

Fig. 6. The mean value of ΔI_{dlin} vs. time calculated for different σ_d.

Since the parameter d_{ox} may fluctuate, one should consider the mean value of ΔI_{dlin} and its standard deviation as functions of time:

$$<\Delta I_{dlin}>(t) = \int \Delta I_{dlin}(d_{ox},t) D(d_{ox},d_n,\sigma_d)\delta d_{ox} \quad (5)$$
$$\sigma^2_{\Delta Idlin}(t) = \int [\Delta I_{dlin}(d_{ox},t) - \Delta I_{dlin}(d_n,t)]^2 D(d_{ox},d_n,\sigma_d)\delta d_{ox}$$

where D is the distribution of the oxide thickness and σ_d the standard deviation. As an example, we evaluated these dependences for situations when d_{ox} obeys Gaussian and uniform distributions. In the first case the standard deviation of the oxide thickness was σ_d = 5%, 10%, 20%, and 30% of d_n. In the second case we assumed that d_{ox} is homogeneously distributed in the interval of $[d_{ox}-3\sigma_d; d_{ox}+3\sigma_d]$ with σ_d having the same values as in the first case (in the case of uniform distribution with such a span, the standard deviation, of course differs from σ_d). The results are presented in Figs. 6,7. Notwithstanding the fact that $\Delta I_{dlin}(t)$ is very sensitive to d_{ox} variations (Fig. 5) the mean value $\langle\Delta I_{dlin}\rangle(t)$ substantially differs from the nominal one (i.e. calculated for the fixed value $d_{ox} = d_n$) only in the case of a wide uniform distribution, see Fig. 6. Fig. 7 demonstrating rather low $\Delta I_{dlin}(t)$ dispersions at all stress times also confirms this trend.

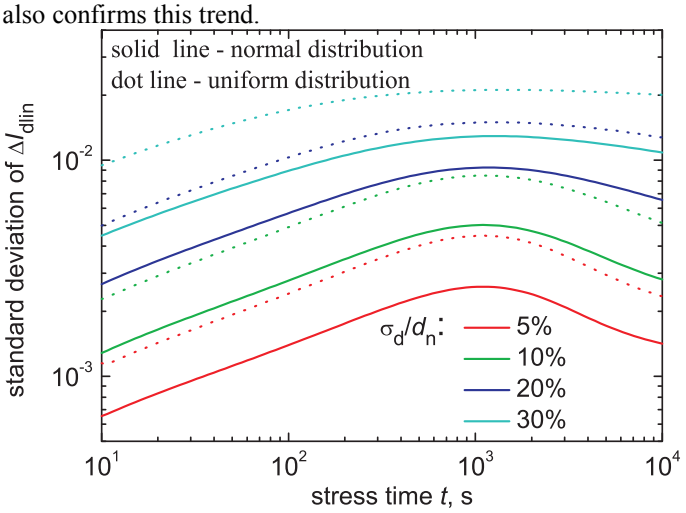

Fig. 7. The standard deviation of $\Delta I_{dlin}(t)$ calculated for different σ_d.

IV. Conclusion

Using the TCAD version of our physics-based model of hot-carrier degradation we calculated a series of carrier acceleration integrals for devices of identical architecture but with different oxide thicknesses. Then we have incorporated the information how the acceleration integral changes with d_{ox} into our analytical approach to HCD modeling. We find that only two parameters in the AI analytical formula change with d_{ox}. Their dependences on d_{ox}/d_n have been represented by fitting expressions covering the whole range of d_{ox}/d_n variations. This fitting allows to avoid time consuming Monte-Carlo simulations while studying HCD in devices with different d_{ox}.

We have analyzed the impact of oxide thickness variations on the linear drain current change vs. time during hot-carrier stress. The calculations have demonstrated that $\Delta I_{dlin}(t)$ is rather sensitive to an oxide thickness change at short and moderate stress times. For longer stress times, the difference between ΔI_{dlin} obtained for different oxide thicknesses tends to vanish. This is because at long times all Si-H bonds in the vicinity of the acceleration integral peak are predominately broken independently on d_{ox}. As an example, we have also calculated the mean value and the standard deviation of $\Delta I_{dlin}(t)$ for different d_{ox} distributions.

Acknowledgment

This work has obtained the financial support from the EC's FP7 Grant agreement No. 216436 (ATHENIS) and from the ENIAC MODERN Project No. 820379, from the Austrian Science Fund (FWF) project No. P23958, and from EC's FP7 grant agreement NMP.2010.2.5-1 (MORDRED).

References

[1] S. Cristoloveanu, H. Haddara, N. Revil, "Defect localization induced by hot carrier injection in short-channel MOSFETs: concept, modeling, and characterization", Microel. Reliab., vol. 33, pp. 1365-1385 (1993).

[2] A. Acovic, G. LaRosa, Y.-Ch. Sun, "A review of hot-carrier degradation mechanisms in MOSFETs", Microel. Reliab, vol. 36, pp. 845-869 (1996).

[3] S. Mahapatra, Ch.D. Parikh, V.R. Rao, Ch.R, Viswanathan, J. Vasi, "Device scaling effects on hot-carrier induced ibreface and oxide-trapped charge distributions in MOSFETs", IEEE Trans. Electron Dev., vol. 47, pp. 789-796 (2000).

[4] S. Rauch, G. La Rosa, "CMOS Hot Carrier: From Physics to End Of Life Projections, and Qualification", IRPS-2010, tutorial.

[5] A. Bravaix, V. Guard, "Hot-carroer degradation issues in advanced CMOS modes" ESREF-2010, tutorial.

[6] S.E. Tyaginov, I.A. Starkov, H. Enichlmair, J.M. Park, Ch. Jungemann, T. Grasser, in: "Silicon Nitride, Silicon Dioxide, and Emerging Dielectrics"; ECS Transactions 2011, pp. 321-352 (2011).

[7] I. Starkov, S. Tyaginov, H. Enichlmair, J. Cervenka, S. Carniello, J.M. Park, H. Ceric, T. Grasser, "Hot-carrier degradation caused interface state profile – simulations versus experiment", Journ. Vacuum Sci. Techn. B, vol. 29, pap. No. 01AB09 (2011).

[8] International Technology Roadmap for Semiconductors (ITRS) – 2010.

[9] S. Tyaginov, I. Starkov, H. Enichlmair, Ch. Jungemann, J.M. Park, E. Seebacher, R. Orio, H. Ceric, T. Grasser, "An analytical approach for physical modeling of hot-carrier degradation" Microel. Reliab., vol. 51, pp. 1525-1529 (2011).

[10] C. Jungemann, B. Meinerzhagen, "Hierarchical Device Simulation", Springer Verlag Wien/New York, 2003.

[11] S. Tyaginov, I. Starkov, O. Triebl, J. Cervenka, Ch. Jungemann, S. Carniello, J.M. Park, H. Enichlmair, M. Karner, C. Kernstock, E. Seebacher, R. Minixhofer, H. Ceric, T. Grasser, "Hot-carrier degradation modeling using full-band Monte-Carlo Simulations", IPFA-2010, pp. 341-345 (2010).

[12] MINIMOS-NT Device and Circuit Simulator, User's Guide, Institute for Microelectronic, TU Wien.

[13] Global TCAD Solutions GmbH: http://www.globalTCADsolutions.com

[14] W. McMahon, A. Haggag, K. Hess, "Reliability scaling issues for nanosacle devices", IEEE Trans. Nanotech., vol. 2, pp. 33-38 (2003).

[15] A. Bravaix, C. Guerin, V. Huard, D. Roy, J.M. Roux, E. Vincent, "Hot-carrier acceleration factors for low power management in DC_AC stressed 40nm NMOS node at high temperature", in Proc. IRPS-2009, pp. 531-546 (2009).

[16] W. McMahon, K. Matsuda, J. Lee, K. Hess, J. Lyding, "The effects of the multiple carrier model of interface state generation of lifetime extraction for MOSFETs", 2002 Int. Conf. Mod. Sim. Micro., vol. 1, pp/ 576-579 (2002).